the FEBS Journal

# MicroRNA-133b inhibits the growth of non-small-cell lung cancer by targeting the epidermal growth factor receptor

Lingxiang Liu[1], Xiaoyan Shao[2], Wen Gao[1], Zhi Zhang[3], Ping Liu[1], Rongsheng Wang[1], Puwen Huang[1], Yongmei Yin[1] and Yongqian Shu[1]

1 Cancer Center, The First Affiliated Hospital of Nanjing Medical University, Nanjing, China
2 Department of Hematology, The Affiliated DrumTower Hospital of Nanjing University Medical School, Nanjing, China
3 Department of Thoracic Surgery, The Cancer Hospital of Nanjing Medical University, Nanjing, China

**Keywords**
epidermal growth factor receptor (EGFR); microRNA; miR-133b; non-small-cell lung cancer; targeted therapy

**Correspondence**
Y. Shu, Cancer Center, The First Affiliated Hospital of Nanjing Medical University, No. 300, Guangzhou Rd, Nanjing, Jiangsu Province, China
Fax: +86 25 68136428
Tel: +86 25 68136428
E-mail: shuyongqian@hotmail.com

(Received 28 March 2012, revised 26 July 2012, accepted 7 August 2012)

doi:10.1111/j.1742-4658.2012.08741.x

Both the deregulation of microRNAs and epidermal growth factor receptor (EGFR) are emerging as important factors in non-small-cell lung cancer (NSCLC). Here, miR-133b was found to be associated with tumor stage, the extent of regional lymph node involvement, stage, visceral pleura or vessel invasion and *EGFR* mRNA expression in Chinese patients with NSCLC. Bioinformatic analysis and luciferase reporter assay revealed that miR-133b can interact specifically with the 3′-UTR of *EGFR* mRNA. Functionally, miR-133b transfection showed regulatory activity in translationally repressing *EGFR* mRNA. Moreover, miR-133b transfection may modulate apoptosis, invasion and sensitivity to EGFR-TKI through the EGFR signaling pathways, especially in EGFR-addicted NSCLC cells. Taken together, our findings show that miR-133b can inhibit cell growth of NSCLC through targeting EGFR and regulating its downstream signaling pathway. This finding has important implications for the development of targeted therapeutics for a number of EGFR-addicted cancers.

## Introduction

Lung cancer is the leading cause of cancer-related mortality for both men and women, with 222 520 new cases and 157 300 deaths expected in the USA in 2010 [1]. According to the American Cancer Society, non-small-cell lung cancer (NSCLC) accounts for 85% of lung cancer cases. Despite improvements in diagnosis and therapy, the overall 5-year survival is ~ 15%. Systemic chemotherapy remains only palliative or modestly effective. Recent advances in cancer biology have led to the use of epidermal growth factor receptor (EGFR) tyrosine kinase inhibitors (EGFR-TKIs), including gefitinib and erlotinib. EGFR-TKIs have limited but valuable activity in previously treated NSCLC patients. *EGFR* mutation (exons 18–21), increased *EGFR* copy number or increased expression of EGFR/phosphorylated EGFR (pEGFR) leads to significantly improved response rates to EGFR-TKIs in patients with pretreated NSCLC [2]. These biomarkers are not mutually exclusive, and the expression of EGFR may predict *EGFR* gene status (including copy number and mutation) to some extent [3]. However, it was considered that an increased *EGFR* copy number was possibly associated with not only sensitivity but also resistance to gefitinib [4].

**Abbreviations**
BCL2L2, B-cell CLL/lymphoma 2-like protein 2; CI, confidence interval; EGFR, epidermal growth factor receptor; EGFR-TKI, epidermal growth factor receptor tyrosine kinase inhibitor; ERK, extracellular signal-related kinase; FITC, fluorescein isothiocyanate; GAPDH, glyceraldehyde-3-phosphate dehydrogenase; IC50, 50% inhibitory concentration; ISH, *in situ* hybridization; MCL-1, myeloid cell leukemia 1; miRNA, microRNA; NSCLC, non-small-cell lung cancer; pAKT, phosphorylated AKT; pEGFR, phosphorylated epidermal growth factor receptor; pERK, phosphorylated extracellular signal-related kinase; qRT-PCR, real-time quantitative RT-PCR; SD, standard deviation; snRNA, small nuclear RNA.

MicroRNAs (miRNAs) are tiny, noncoding, endogenous, single-stranded RNAs (18–25 nucleotides) that regulate gene expression. miRNAs are frequently located at fragile sites and genomic regions that are deleted or amplified in cancers, suggesting that miRNAs act as key players in human tumorigenesis. miRNAs bind with imperfect complementarity to the 3′-UTRs of target mRNAs, repressing the expression of these genes at the level of translation [5]. Recently, miRNAs have been associated with tumor invasiveness and metastatic potential, and are thought of as being diagnostic and prognostic markers for several types of cancer, including lung cancer [6], breast cancer [7], chronic lymphocytic leukemia [8], colorectal cancer [9], hepatic cancer [10], pancreatic cancer [11], and prostate cancer [12]. It has also been suggested that miRNAs may constitute a viable tool to augment current therapies in human cancers [13]. Accumulating evidence shows that miRNA may participate in the EGFR network in lung cancer oncogenesis and provide a clue to overcoming EGFR-TKI resistance [6,14].

Because both the deregulation of miRNAs and EGFR are emerging as important factors in NSCLC, we queried whether genomic loss of a miRNA could lead to EGFR overexpression, thereby increasing the sensitivity to or overcoming resistance to EGFR-TKI.

In 27 paired tumor and nontumor lung tissues, miR-133b was found to be associated with tumor, the extent of regional lymph node involvement, stage, visceral pleura or vessel invasion and *EGFR* mRNA expression in Chinese patients with NSCLC. After performing bioinformatic analysis, we showed that miR-133b, an miRNA located on chromosome 6p12.2, may target *EGFR*. Moreover, chromosomal aberrations associated with lung cancer are frequently observed in chromosome 6p11.1–q11, which plays an important role in tumor progression and is associated with histological differentiation [15]. We investigated the ability of miR-133b to regulate EGFR in several NSCLC cell lines, and determined whether miR-133b was associated with growth, apoptosis, invasion or metastasis of NSCLC cells. We also explored the relationship between miR-133b and sensitivity to EGFR-TKI in NSCLC cells.

## Results

### Decreased miR-133b expression is associated with tumor stage, lymph node metastasis, and *EGFR* mRNA levels

To determine the potential clinicopathological implications of altered miR-133b expression, we investigated the expression levels of miR-133b and *EGFR* mRNA in 27 lung cancer tissues and corresponding non-neoplastic lung tissues by real-time quantitative RT-PCR (qRT-PCR). The results demonstrated that miR-133b expression levels in NSCLC tissues were significantly lower than those in paired non-neoplastic lung tissues (*t*-test, $P = 0.002$) (Fig. 1A), and this was confirmed by *in situ* hybridization (ISH) with granular brown cytoplasmic positive staining (Fig. S1). Correlations between miR-133b expression levels and the clinicopathological characteristics of NSCLC are summarized in Tables 1 and S1. A significant inverse correlation was found between miR-133b levels and *EGFR* mRNA transcript levels ($r = -0.71$, $P = 0.000$) (Fig. 1B). Notably, we also found negative correlations between

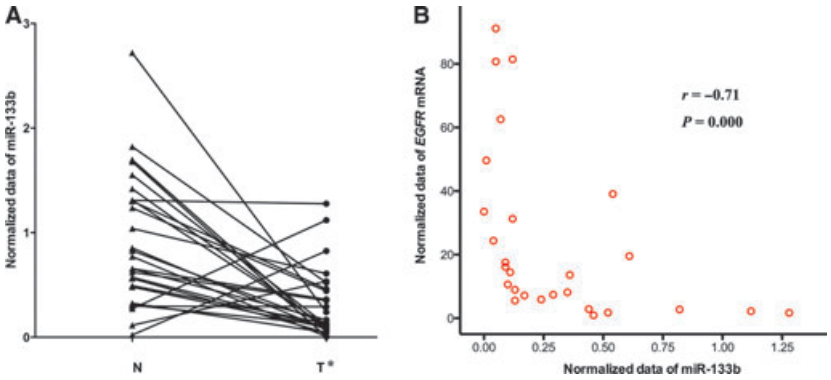


**Fig. 1.** Expression of miR-133b was downregulated and inversely correlated with EGFR expresssion in NSCLC. (A) miR-133b expression was measured by qRT-PCR in 27 matched NSCLC and normal bronchial tissues. All data were normalized to those of U6 snRNA. Data are represented as a before-and-after plot. Lines indicate mean expression. T, tumor tissue; N, normal tissue. $*P < 0.001$, paired Student's *t*-test. (B) miR-133b and EGFR expression correlated inversely in 27 matched NSCLC cancer and normal bronchial tissues. miR-133b and *EGFR* mRNA were measured by qRT-PCR. Correlation analysis showed a significant relationship between these factors (Spearman $r = -0.71$; $P = 0.000$).

**Table 1.** Comparison of several clinicopathological factors and expression levels of miR-133b in NSCLC specimens (chi-square test). The expression levels of miR-133b in 27 matched NSCLC cancer and normal bronchial tissues were measured by qRT-PCR. Because the amplification efficiency was close to 100%, the relative amount of each miR-133b/U6 snRNA was given by $2^{-\Delta\Delta Ct}$, as described by Livak and Schmittgen. The median relative expression level of miR-133b was 0.134-fold of normal. Thus, 14 patients had low miR-133b expression (< 0.134) and 13 patients had high miR-133b expression (> 0.134). Clinical stage was defined acccording to the IASLC Lung Cancer Staging Project (2007). AC, adenocacinoma; RUL, right upper lobe; SC, squamous cell carcinoma; VPI/VI, visceral pleura invasion or vessel invasion.

| | | miR-133b | | |
|---|---|---|---|---|
| Parameter | *N* | Low expression | High expression | *P*-value[a] |
| Sex | | | | |
| Male | 16 | 8 | 8 | |
| Female | 11 | 6 | 5 | 1 |
| Age (years) | | | | |
| ≤ 63 | 12 | 6 | 6 | |
| > 63 | 15 | 8 | 7 | 1 |
| Clinical stage | | | | |
| I | 14 | 5 | 9 | 0.128 |
| II–IV | 13 | 9 | 4 | |
| Histological grade | | | | |
| Well/moderately differentiated | 16 | 10 | 6 | |
| Poorly differentiated | 11 | 4 | 7 | 0.252 |
| Tumor diameter (cm) | | | | |
| ≤ 5 | 21 | 12 | 9 | |
| > 5 | 6 | 2 | 4 | 0.215 |
| Lymph node | | | | |
| Positive | 10 | 9 | 1 | |
| Negative | 17 | 5 | 12 | 0.004 |
| Smoking status | | | | |
| Never smoker | 13 | 6 | 7 | |
| Current or former smoker | 14 | 8 | 6 | 0.706 |
| VPI/VI | | | | |
| Yes | 11 | 8 | 3 | |
| No | 16 | 6 | 10 | 0.120 |
| Location | | | | |
| Non-RUL | 18 | 10 | 8 | |
| RUL | 9 | 4 | 5 | 0.695 |
| Histology | | | | |
| AC | 19 | 10 | 9 | |
| SC | 8 | 4 | 4 | 1 |

[a] Fisher's exact test.

miR-133b expression levels and the extent of regional lymph node involvement ($r = -0.62$, $P = 0.001$), stage ($r = -0.50$, $P = 0.007$), and visceral pleura or vessel invasion ($r = -0.44$, $P = 0.023$). Meanwhile, a positive correlation was found between *EGFR* mRNA levels and the extent of regional lymph node involvement ($r = 0.54$, $P = 0.004$). The expression of miR-133b was not associated with any other clinicopathological characteristics of patients with NSCLC (sex, age, smoking index, histology, cell differentiation, size and location of the tumor) in our study. The median follow-up time for the entire cohort was 396 days (range, 235–618 days), no significant correlation was found between miR-133b expression levels and overall survival time of NSCLC patients (Fig. S2).

## miR-133b targets EGFR by binding to the *EGFR* 3′-UTR

To determine whether miR-133b targets the *EGFR* 3′-UTR (GenBank ID: NM_005228), TARGETSCAN 5.2 and PICTAR were used to assess the complementarity of miR-133b to the *EGFR* 3′-UTR. It was shown that *EGFR* mRNA contained an miR-133b seven-nucleotide seed match at position 50–56 of the *EGFR* 3′-UTR. (Fig. S3A) Functional annotation analysis of other cancer-related genes targeted by miR-133b showed that the enriched functional categories were regulation of gene expression, the intracellular organelle, protein binding, etc. (Table S2).

To determine whether or not miR-133b directly recognizes the *EGFR* 3′-UTR, we amplified a sequence of the 3′-UTR of *EGFR* mRNA with the predicted target sites of miR-133b from human genomic DNA, and then inserted the resulting amplicon into the pMIR-Report-Luc plasmid. Transfection of miRNA-133b and EGFR@pMIR-Report-Luc plasmid into HEK 293T cells led to a 49.4% ($P = 0.03$) reduction in normalized luciferase values as compared with controls including pRL-TK reporter plasmids (Fig. S3B). These data suggest that miR-133b directly inhibits *EGFR* expression via its 3′-UTR.

## miR-133b is regulated by liposomal delivery of mimic or inhibitor

miR-133b mimic was transfected by the use of cationic liposomes into lung cancer cells. To assess the efficiency of our miR-133b transfection, an miR-133b activity reporter plasmid, containing the above fully complementary miR-133b target sites as a 3′-UTR for the luciferase gene, was used. Transfection with miR-133b ablated reporter activity, indicating high transfection efficiency (Fig. S4A).

After transfection, miR-133b expression in H1650, A549, H1975 and PC-9 cells was significantly increased by 72.1% [95% confidence interval (CI) 40.9–110.2%), 54.2% (95% CI 30.1–82.7%), 653.9% (95% CI 521.2–815.0%), and 72.7% (95% CI 32.6–105.3%), respectively, as compared with each cell line transfected with

miR-NC. After transfection with miR-133b inhibitor, miR-133b expression in H1650, A549, H1975 and PC-9 cells was significantly decreased by 52.5% (95% CI 44.7–59.2%), 45.4% (95% CI 38.5–51.5%), 43.2% (95% CI 24.8–57.1%), and 50.7% (95% CI 36.2–61.9%), respectively, as compared with control (Fig. S4B).

### miR-133b induces apoptosis of NSCLC cells

After treatment of H1650, A549, H1975 and PC-9 cells with miR-133b mimic, the increased percentages of apoptotic lung cancer cells as compared with control were 27.9% (95% CI 26.3–29.4%), 27.0% (95% CI 25.3–28.5%), 24.6% (95% CI 23.3–25.9%), and 37.2% (95% CI 36.2–38.2%), respectively. Treatment with miR-133b inhibitor for 48 h also resulted in increased apoptosis and increased numbers of necrotic cells in the four cell lines. Differences in apoptotic cell numbers between transfectants and control in H1650, A549, H1975 and PC-9 cells, respectively, were 6.7% (95% CI 5.0–8.3%), 10.7% (95% CI 9.4–12.0%), 10.5% (95% CI 9.4–11.5%), and 12.9% (95% CI 11.7–14.1%). All *P*-values for the differences between the miR-133b mimic/inhibitor and the control were $< 0.05$ (Fig. 2A).

### miR-133b enhances sensitivity to gefitinib in NSCLC cells

To study whether miR-133b could regulate the sensitivity to gefitinib in NSCLC cells, they were treated with gefitinib after being transfected with miR-133b mimic, miR-133b inhibitor, and miR-NC. The survival rates are shown in Fig. 2B. The 50% inhibitory concentration (IC50) values of gefitinib were 8.71 μM (95% CI 6.10–12.44), 6.76 μM (95% CI 4.62–9.90), 21.10 μM (95% CI 15.11–29.46), and 0.02 μM (95% CI 0.02–0.03), respectively, for H1650, A549, H1975 and PC-9 cells. The IC50 values of gefitinib after transfection with miR-133b inhibitor were 9.02 μM (95% CI 7.30–11.13), 13.71 μM (95% CI 11.33–16.59), 30.79 μM (95% CI 23.38–40.55), and 0.61 μM (95% CI 0.48–0.77), respectively, for H1650, A549, H1975 and PC-9 cells. The IC50 values of gefitinib after transfection with miR-133b mimic were 1.04 μM (95% CI 0.92–1.18), 4.13 μM (95% CI 3.42–4.99), 5.66 μM (95% CI 4.25–7.54), and 0.02 μM (95% CI 0.01–0.02), respectively, for H1650, A549, H1975 and PC-9 cells. Significant resistance to gefitinib was found in A549, H1975 and PC-9 cells transfected with miR-133b inhibitor as compared with controls ($P < 0.05$). Significantly more sensitivity to gefitinib was found in H1650, H1975 and PC-9 cells transfected with miR-133b mimic than in controls ($P < 0.05$) (Fig. 2C). After application of miR-133b mimic, A549 cells with the highest relative expression of miR-133b were not more sensitive to gefitinib. After application of miR-133b inhibitor, H1650 cells with the lowest relative expression of miR-133b were not more resistant to gefitinib. The different responses to miR-133b mimic and inhibitor were partially attributed to the different expression levels of miR-133b.

### miR-133b inhibits invasion of NSCLC cells

In the invasion assay, ectopic expression of miR-133b resulted in 13.3%, 13.8%, 8.7% and 48.4% decreases, respectively, in H1650, A549, H1975 and PC-9 cell invasiveness. Moreover, the loss of miR-133b promoted the invasion and metastasis of NSCLC cells: 7.5%, 23.1%, 20.2% and 147.7% for H1650, A549, H1975 and PC-9 cells, respectively. Stronger regulation was found in PC-9 and A549 cells, which were highly or moderately addicted to the EGFR signaling pathway respectively (Fig. 3).

### miR-133b suppresses the expression of EGFR

Although *EGFR* was identified as a target gene for miR-133b, it was unknown whether miR-133b could regulate endogenous EGFR expression. NSCLC cells were transfected with miR-133b mimic, miR-133b inhibitor or miR-NC to determine whether miR-133b could modulate endogenous EGFR. As compared with control, the level of *EGFR* mRNA detected by qRT-PCR was not significantly changed in H1650, A549 and H1975 cells (Fig. 4A). In PC-9 cells, which are EGFR-addicted lung cancer cells, *EGFR* mRNA was significantly downregulated by transfection with miR-133b mimic. Additionally, the EGFR level was measurably reduced by miR-133b mimic and increased by miR-133b inhibitor (Fig. 4B). These data show that endogenous EGFR expression was regulated by miR-133b.

### miR-133b suppresses EGFR pathway activation

To examine the potential relationship between miR-133b and EGFR signaling, the expression of pEGFR (Tyr1068) and the expression of downstream signaling molecules were measured by western blotting. Consistent with previous observations, miR-133b mimic abolished the phosphorylation of EGFR, AKT and extracellular signal-related kinase (ERK)1/2 in the EGFR-addicted PC-9 and A549 cells. However, in H1650 and H1975 cells, which were not EGFR-

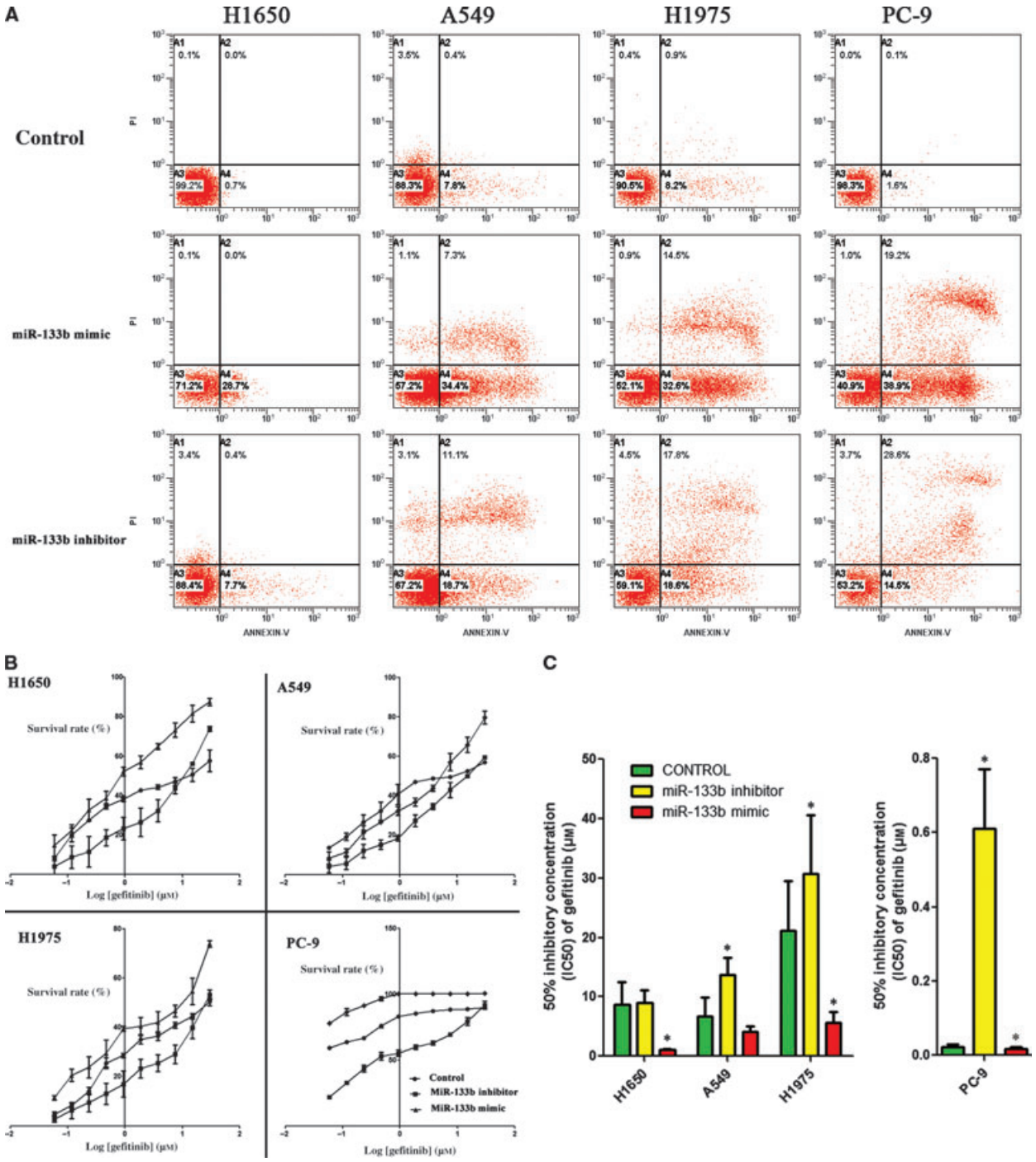


**Fig. 2.** miR-133b inhibited the proliferation of lung cancer cells. (A) miR-133b induced apoptosis in lung cancer cells. After 48 h of incubation in the presence of control, miR-133b mimic, or miR-133b inhibitor, total cell lysates were stained with annexin V–FITC and propidium iodide (PI), and this was followed by flow cytometric analysis. miR-133b strengthened apoptosis in lung cancer cells, especially for EGFR-addicted cells. Data are expressed as mean ± SD from three independent experiments. (B, C) miR-133b strengthened the sensitivity to gefitinib. Lung cancer cells were transfected with 10 nM miR-133b mimic, miR-133 inhibitor, or a negative control. (B) Log[inhibitor]-normalized response to gefitinib in NSCLC cells. (C) The IC50 values of gefitinib in NSCLC cells after transfection with miR-133b mimic, miR-133 inhibitor, or a negative control. Means (bars) and 95% CIs (error bars) are shown. $*P < 0.05$ as compared with control.

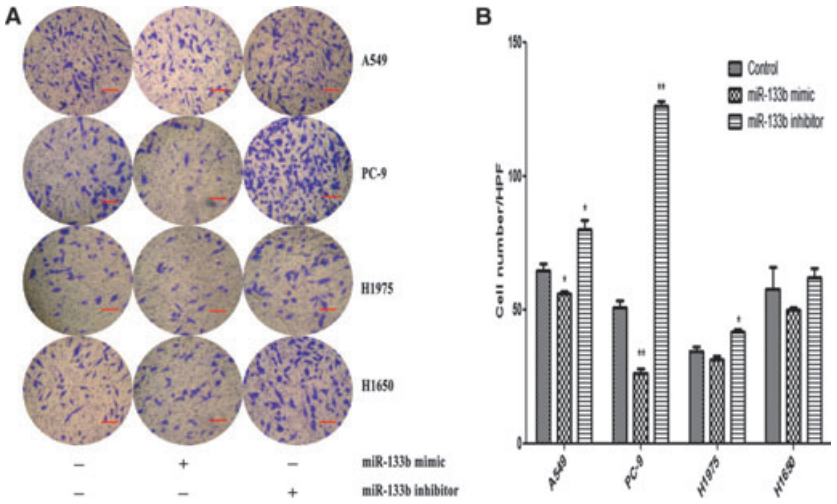


**Fig. 3.** miR-133b suppressed lung cancer cell invasion. Lung cancer cells were transfected with 10 nM miR-133b mimic, miR-133 inhibitor, or a negative control. (A) Representative fields of invasive cells on the membrane. (B) Average invasive cell numbers were from three independent experiments ± SD. $*P < 0.05$ as compared with control. HPF, high-power field.

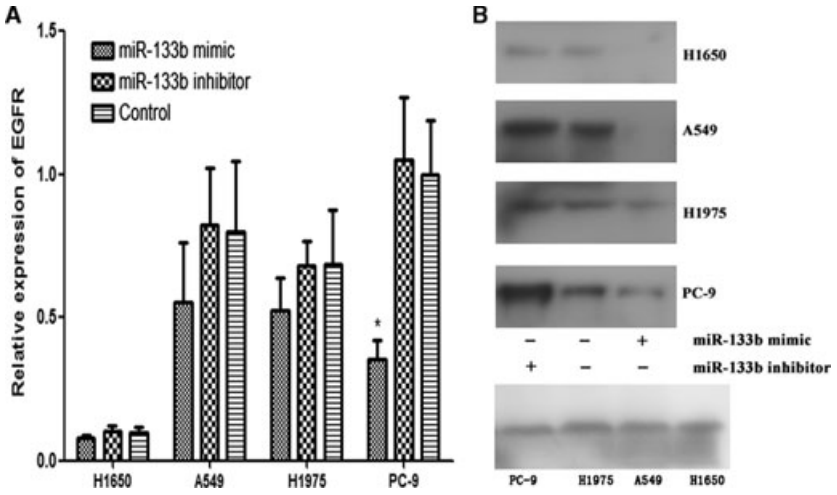


**Fig. 4.** miR-133b suppressed EGFR expression. Lung cancer cells were transfected with 10 nM miR-133b mimic, miR-133 inhibitor, or a negative control. *EGFR* mRNA expression, measured by qRT-PCR, was normalized to *GAPDH* expression. EGFR expression was detected by western blotting and quantified by densitometry relative to β-actin expression. Data are shown as the mean ± SD from three independent assays. $*P < 0.05$ as compared with control.

addicted NSCLC cell lines, no definite changes in the expression of pEGFR, phosphorylated AKT (pAKT) and phosphorylated ERK (pERK)1/2 were found after transfection with miR-133b mimic or inhibitor (Fig. 5). A flow diagram of the miR-133b regulation of EGFR and links to related pathway is shown in Fig. S5.

## Discussion

Although a role for miRNAs in cancer has been postulated, the molecular mechanisms by which miRNA can regulate tumor growth or invasion have not been established. In this study, we found that the expression of miR-133b was apparently decreased in NSCLC tissues and cells, and had a negative relationship with stage and visceral pleura or vessel invasion in NSCLC. Our findings were consistent with the reduced expression of miR-133b in lung cancer found in previous study [16]. To our knowledge, this is the first report showing that miR-133b inhibits the growth and invasion of NSCLC cells by targeting *EGFR* and repressing EGFR signaling, especially in EGFR-addicted

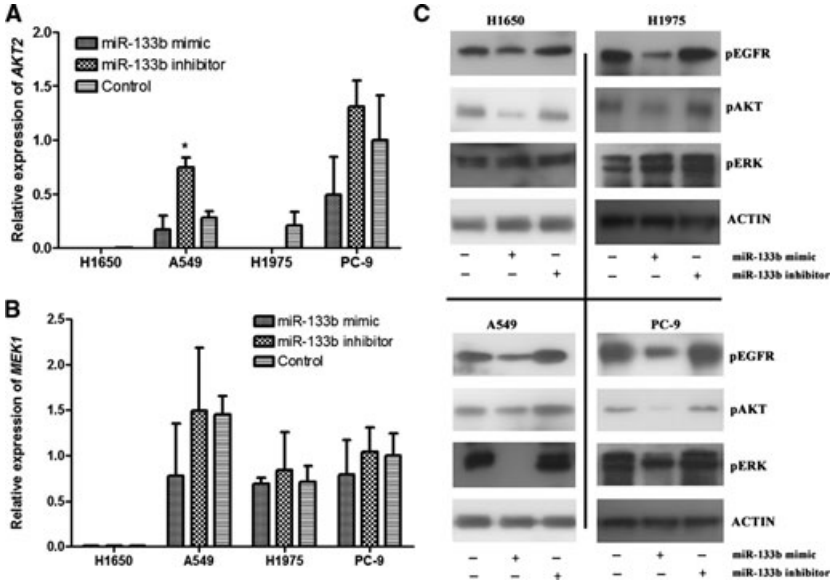


**Fig. 5.** The EGFR signaling pathway was downregulated in miR-133b-overexpressing lung cancer cells. Lung cancer cells were transfected with 10 nM miR-133b mimic, miR-133 inhibitor, or a negative control. (A) *AKT2* mRNA expression and (B) *MEK1* mRNA expression, measured by qRT-PCR, was normalized to *GAPDH* expression. (C) pEGFR, pAKT and pERK expression was detected by western blotting and quantified by densitometry relative to β-actin expression. Data are shown as the mean ± SD from three independent assays. $*P < 0.05$ as compared with control.

lung cancer cells. Moreover, miR-133b can restore or enhance EGFR-TKI sensitivity in NSCLC cells. These results suggest that the expression of miR-133b might be implicated in the progression and phenotype of NSCLC.

It is now well known that miRNAs regulate the expression of multiple target genes and affect a variety of cellular pathways. miR-133b, located on chromosome 6p12.2, has been studied in midbrain dopamine neurons [17], cardiomyocytes [18], skeletal muscles [19], extraocular muscles [20], myoblasts [21], osteoblasts [22], T-helper cells [23], and coronary artery disease [24]. More recently, miR-133b has been suggested to function as a tumor suppressor gene, because it was shown to be downregulated in several cancer types as compared with normal tissues, including lung cancer [25], esophageal squamous cell carcinoma [26], colorectal cancer [27], gastric cancer [28], bladder cancer [29], squamous cell carcinoma of the tongue [30], cervical carcinoma [31], breast cancer, lymphoma, ovarian cancer, prostate cancer, and testicular cancer [32].

Functionally, miR-133b targets the prosurvival molecules myeloid cell leukemia 1 (*MCL-1*) and B-cell CLL/lymphoma 2-like protein 2 (*BCL2L2*) in lung cancer [16], oncogenic fascin homolog 1 gene in esophageal squamous cell carcinoma [26], the proto-oncogene *c-MET* in colorectal cancer [33], the potential oncogene pyruvate kinase type M2 in squamous cell carcinoma of the tongue [30], and the anti-oncogene *MST2* and the small GTPases *RhoA* and *CDC42* in cervical cancer, affecting cell proliferation and invasion. Moreover, elevation of miR-133b deregulates the AKT1 and ERK signaling pathways via direct effects on MST2, CDC42 and RhoA activities [31]. These data suggest that miR-133b may be involved in the pathology of cancer by targeting distinct pathways that are specific for each disease [34] (Fig. S5).

However, it largely remains unclear which of these pathways miR-133b affects and how it does so, in particular regarding miRNA-related oncogenesis, because little is known about the physiological targets of miR-133b. Multiple lines of evidence indicate that EGFR is one such target. First, miR-133b level inversely correlated with EGFR expression in NSCLC tumor samples. Second, the ability of miR-133b to regulate EGFR expression may be direct, as it binds to the 3′-UTR region of EGFR transcript with complementarity to the seed region of miR-133b. Third, EGFR@pMIR-Report-Luc is specifically responsive to miR-133b mimic. Fourth, EGFR expression is decreased in lung cancer cells treated with miR-133b mimic, and increased in those treated with miR-133b inhibitor. Finally, miR-133b can regulate EGFR signaling and restore/enhance EGFR-TKI sensitivity, especially in EGFR-addicted lung cancer cells. Although miRNAs may inhibit translation and/or

accelerate mRNA degradation [35], our results suggested that miR-133b inhibited EGFR protein translation, and *EGFR* mRNA levels were not significantly affected by miR-133b mimic or inhibitor.

The EGFR family, including four distinct transmembrane receptors (EGFR/erbB-1, HER2/erbB-2, HER3/erbB-3, and HER4/erbB-4), is expressed in many tumors, and is regarded as a biomarker of aggressive disease and shorter survival [36]. As an oncogene protein, it has led to the development of anticancer therapeutics directed against EGFR, including gefitinib.

Activation of EGFR causes increased cell proliferation, decreased apoptosis, and enhanced tumor cell motility and neo-angiogenesis. As described above, miR-133b also targets the prosurvival genes *MCL-1* and *BCL2L2* in lung cancer and induces apoptosis. However, we conducted more experiments (apoptosis, sensitivity to gefitinib, and invasion assay) with EGFR, and found that their effects (apoptosis, sensitivity to gefitinib, and invasion) are much more significant when miR-133b mimic or inhibitor is applied, especially on EGFR-addicted lung cancer cells. This may also suggest that the impact of miR-133b on cell proliferation and invasion was probably mediated by targets beyond EGFR, and was partially caused by MCL-1 and BCL2L2, especially on non-EGFR-addicted lung cancer cells. The tyrosine phosphorylation of EGFR leads to the activation of many signaling pathways through the recruitment of diverse proteins. For example, AKT acts downstream of phosphatidylinositol-3 kinase to regulate tumor cell proliferation and invasion [37]. At the same time, the RAF–mitogen-activated protein kinase–ERK pathway can also communicate signals from EGFR on the surface to the DNA in the nucleus of the cell. Also, substrate-level phosphorylation by ERK may promote proliferation, invasion, differentiation, and cellular survival [38,39]. Therefore, the identification of *EGFR* as an miR-133b target gene provides a possible explanation for why downregulated miR-133b can drive tumorigenesis [26] and invasion [27].

In the present study, we used four lung cancer cell lines with overexpressed EGFR or tyrosine kinase domain-mutated EGFR to determine the association of miR-133b with the EGFR signaling pathway. In the three EGFR-mutant cell lines (PC-9, H1650, and H1975 cells), high levels of pEGFR were found with induction of pAKT. Furthermore, EGFR with activating mutations was seen to activate the AKT pathway rather than the ERK pathway in the current study. As previously reported [40], we also found that NSCLC cells with high-level expression of pAKT (PC-9 cells) had a better response rate to EGFR-TKI. However, in A549 cells with wild-type EGFR, the ERK pathway was probably regulated after transfection with miR-133b. PC-9 and A549 cells, which are highly and intermediately sensitive to EGFR-TKI, respectively, were considered to be the so-called EGFR-addicted cells [41] in this study. It was found that the EGFR-addicted cells were more sensitive to miR-133b mimic/inhibitor transfection than non-EGFR-addicted cells with regard to apoptosis induction, cell invasion, EGFR-TKI sensitivity, and EGFR pathway activity. More importantly, relative EGFR expression in PC-9 cells was only slightly enhanced (5%) by miR-133b inhibition (Fig. 4A), whereas the corresponding lung cancer cell invasion was significantly increased (2.47-fold) (Fig. 3A). This demonstrates that the slight change in EGFR level in EGFR-addicted cancer cells can greatly affect the final outcome of cancer cells. Taken together, our data strongly suggest that miR-133b can functionally regulate the EGFR signaling pathway.

Although there were many controversial roles in the functional regulation of microRNA, microRNA might be selected cancer's ultimate Achilles heel through modulating the crucial pathway, similar to targeted therapy by EGFR-TKI in NSCLC [42]. Our results from the chemosensitivity and apoptosis assays also indicated that miR-133b may enhance/restore sensitivity to EGFR-TKI. Consequently, multitargeted therapy will overcome primary or acquired resistance to EGFR-TKI [43,44].

In conclusion, we observed that low expression of miR-133b was significantly associated with tumor tissues, stage and invasion as compared with matched normal tissues in Chinese NSCLC patients. All of these findings suggest that miR-133b regulates cell growth, invasion and apoptosis by targeting EGFR. Moreover, they also suggest that transfection of miR-133b has therapeutic potential for overcoming resistance to EGFR-TKI in EGFR-addicted NSCLC. Thus, characterization of the miRNA modulating the EGFR pathway has provided important information with regard to understanding the mechanisms of action of EGFR-TKI in NSCLC cells and optimizing combination targeted therapy to improve its efficacy in the clinic. Nonetheless, our results should be confirmed by *in vivo* and well-designed prospective studies.

## Experimental procedures

### Human lung cancer tissue specimens

All paired tumor and nontumor lung tissues were obtained from patients in the First Affiliated Hospital and the Cancer Hospital of Nanjing Medical University in Nanjing

China from June 2010 to November 2011. The study methodologies conformed to the standards set by the Declaration of Helsinki, and the study was approved by the Institutional Review Board of the First Affiliated Hospital of Nanjing Medical University. Written informed consent was obtained from patients for all of the samples. Tumors were staged according to the 7th edition of the TNM staging system of the American Joint Committee on Cancer (2007) [45]. Tumor histologic grade was assessed according to the World Health Organization criteria [46]. All tissues were stained with hematoxylin and eosin for histological validation and tumor cell evaluation by a pathologist (Fig. S5). Only those cases with > 60–70% tumor cells in the section were used in this study. We also evaluated the size and the quality of samples and the completeness of patient information. Finally, 27 paired lung cancer samples and their corresponding normal lung tissues were selected. All tissues were snap-frozen and stored at −80 °C.

## Characteristics of cell lines and cell assays

H1650, A549, PC-9 and 293T cell lines were obtained from Shanghai Cell Bank, Chinese Academy of Sciences, and the H1975 cell line was purchased from the American Type Culture Collection (ATCC, Manassas, VA, USA). The different features of the four lung adenocarcinoma cell lines are shown in Table 2 [47,48]. The cells were routinely maintained in RPMI-1640 medium (Gibco, Carlsbad, CA, USA) supplemented with 10% fetal bovine serum (Gibco) as protein source, 100 $U \cdot mL^{-1}$ penicillin sodium and 100 $mg \cdot mL^{-1}$ streptomycin sulfate at 37 °C. 293T cells were cultured in DMEM supplemented with 10% fetal bovine serum. An atmosphere of 5% carbon dioxide in air was maintained in a humidified carbon dioxide incubator. The cells were used in the logarithmic phase of growth throughout each experiment. Transfections with hsa-miR-133b mimics, has-miR-133b inhibitor and negative control (miR-NC, cel-miR-67) were performed at a concentration of 20 nM with Lipofectamine 2000 (Invitrogen, Carlsbad, CA, USA). The miR-133b mimic, miR-133b inhibitor and miR-NC were designed and provided by Ambion (Austin, TX, USA).

**Table 2.** The different features of the four lung adenocarcinoma cell lines. PTEN, phosphatase and tensin homolog.

| Cell line | *EGFR* mutations | Sensitivity to EFGR-TKI | Levels of EGFR addiction |
|---|---|---|---|
| H1650 | Exon 21 L858R; Exon 19 del E746–A750; PTEN loss | Primary resistance | Nonaddicted |
| A549 | Wild type | Intermediate sensitivity | Intermediate |
| H1975 | Exon 21 L858R; Exon 19 del E746–A750; Exon 20 T790M | Acquired resistance | Nonaddicted |
| PC-9 | Exon 19 del E746–A750 | High sensitivity | High |

## Bioinformatics analysis and luciferase reporter assay

The search for the potential miR-133b targets on EGFR (accession no. NM_005228) was performed on the following websites for microRNA: TARGETSCAN (http://www.targetscan.org/) and PICTAR (http://pictar.mdc-berlin.de/). Approximately 50 bp of the 3′-UTR of human *EGFR* mRNA encompassing the nucleotide sequence complementary to the miR-133b seed sequence was cloned into the pMIR-REPORT miRNA Expression Reporter Vector System (Ambion). Total RNA (1 μg) was reverse transcribed into cDNA as described above, and the 3′-UTR was amplified with the following primers: forward, 5′-GTGCAAGGACACCTGCCCCC-3′; and reverse, 5′-CACAGGCTCGGACGCACGAG-3′. Purified DNA was digested with *Hin*dIII and *Sac*I (NEB; New England Biolabs, Hitchin, UK). After construction of the EGFR@pMIR-Report-Luc plasmid (reporter plasmid), DNA sequences of the 3′-UTR were verified. For the luciferase assay, 293T HEK and PC-9 cells ($2 \times 10^5$ per well) were plated in each well of a 96-well culture plate and allowed to attach overnight. The cells were cotransfected with 0.1 μg of EGFR@pMIR-Report-Luc plasmid or pRL-TK reporter plasmid (Promega, Madison, WI, USA) and with miR-133b mimic or miR-NC (cel-miR-67), using Lipofectamine 2000 (Invitrogen) on the following day. Forty-eight hours later, the cells were lysed and assayed for firefly and *Renilla* luciferase activity with Dual Luciferase Assay reagent (Promega). Activities were reported as ratios of firefly luciferase to *Renilla* luciferase. Each treatment was performed in triplicate in three independent experiments.

## Drugs and chemicals

Gefitinib was purchased from AstraZeneca (Macclesfield, UK). One gram of gefitinib (C22H24ClFN4O3, WM 446.9) was dissolved in 1 mL of dimethylsulfoxide and stored at −20 °C. Antibody against EGFR (C74B9) and antibody against pEGFR (Tyr1068, 1H12) were purchased from Cell Signaling Technology (Beverly, MA, USA). Antibodies against pERK1/2 (Y204) were from Bioworld Technology (Minneapolis, MN, USA). Antibodies against pAKT1/2/3 (Ser473) were from Santa Cruz (Santa Cruz, CA, USA).

## qRT-PCR

The lung cancer cells were transfected with miR-133b mimic, miR-133 inhibitor or miR-NC in 24-well plates ($2 \times 10^5$ cells per well) for 48 h. Total RNA was prepared with Trizol, and reverse transcribed with the PrimerScript RT reagent Kit (TaKaRa Bio, Otsu, Japan) from cells and

samples of patients. The mRNA and miRNA levels were analyzed by use of SYBR Green Realtime PCR Master Mix with gene-specific primers (Table S3) on the ABI 7500 Fast Real-Time PCR System, according to the manufacturer's instructions. The cycle number at which the reaction crossed an arbitrarily placed threshold (Ct) was determined for each gene. When the amplification efficiency was close to 100%, the relative amount of each mRNA/glyceraldehyde-3-phosphate dehydrogenase (GAPDH) and miR-133b/U6 small nuclear RNA (snRNA) was given by $2^{-\Delta\Delta Ct}$, as described by Livak and Schmittgen [49], where $\Delta Ct = Ct_{mRNA} - Ct_{GAPDH\ mRNA}$ and $\Delta Ct = CtmiR\text{-}133b - Ct_{U6}$ snRNA) respectively, and $\Delta\Delta Ct = \Delta Ct_{experiment} - \Delta Ct_{control}$. Otherwise, when the efficiency was not close to 100%, the relative expression levels were calculated according to the efficiency corrected approach described by Pfaffl *et al.* [50]. All experiments were performed in triplicate.

## ISH

ISH with double-Dig-labeled miR-133b miRCURY LNA probe (Exiqon, Woburn, MA, USA) was performed on formalin-fixed paraffin-embedded samples of paired tumor and nontumor lung tissues essentially according to the manufacturer's instructions. Sections were deparaffinized in xylene, and then rehydrated through a series of ethanol dilutions at room temperature. After the slides had been incubated with PCR-grade Proteinase-K (Roche, Indianapolis, IN, USA) for 10 min at 37 °C, washed stringently with NaCl/$P_i$, and dehydrated in a gradient of ethanol solutions, the hybridization was performed with 40 nM miR-133b doubled-labeled LNA probe for 1 h at 56 °C. Then, sections were washed in decreasing SSC concentrations and incubated with blocking solution for 15 min. For immunostaining, sections were incubated for 30 min with 1 : 250 mouse anti-Dig IgG1 (Roche), and then incubated with labeled polymer-horseradish peroxidase anti-mouse IgG (Dako EnVision+, Glostrup, Denmark) for 30 min at room temperature. 3,3-Diaminobenzidine was applied, and nuclei were counterstained with Carazzi's hematoxylin. The same protocol was used for the negative control, without probe and with scrambled probe. The sections were scored independently by two investigators. The scoring was 0–3, as follows: 0, negative; 1, weak; 2, moderate, and 3, strong.

## Flow cytometry analysis

The lung cancer cell density was adjusted to (0.3–1.0) $\times$ $10^7$ cells·$mL^{-1}$. After serum starvation for 24 h, cells were treated with miR-133b mimic, miR-133b inhibitor or miR-NC for 48 h. A single cell suspension was produced after harvesting with trypsin. The cells were pelleted by centrifugation at 800 ***g*** for 5 min, and washed three times with NaCl/$P_i$. Then cell pellets were then resuspended and fixed with ice-cold 70% ethanol in NaCl/$P_i$, and stored at 4 °C until use. The cells were incubated with RNase A (20 mg·$L^{-1}$; Sigma, St Louis, MO, USA), annexin V–fluorescein isothiocyanate (FITC), and then propidium iodide, according to the manufacturer's recommendations (Annexin V–FITC Apoptosis Detection Kit; Keygen Biotech, Nanjing, China). After incubation for 10 in at room temperature in the dark, the specimens were analyzed on a Coulter XL flow cytometer, with SYSTEM II acquisition software (Beckman Coulter, Miami, FL, USA). The apoptosis rates were calculated. Experiments were conducted at least three times, each with three replicates.

## Cell proliferation and chemosensitivity assay

Lung cancer cells, transfected with miR-133b mimic, inhibitor, and miR-NC, were seeded at a density of 1 $\times$ $10^4$ cells per well in 96-well plates for 48 h. After treatment with different concentrations of gefitinib for 48 h, 20 μL of 5 mg·$mL^{-1}$ 3-(4,5-dimethylthiazol-2-yl)-2,5-diphenyl-tetrazolium bromide (Biosharp, St. Louis, MO, USA) was added to each well and incubated at 37 °C for 4 h. The plates were spun, and the purple-colored formazan precipitates were dissolved in 200 μL of dimethylsulfoxide (Sigma). The absorbance was measured at 490 nm with an automatic multiwell spectrophotometer (Bio-Rad, Hercules, CA, USA). The dose–effect relationship was nonlinear-fitted with curve regression models to obtain the IC50 of gefitinib.

## Cell migration and invasion assay

Transwell chambers (six-well polycarbonate transwell membrane inserts with 8-mm pores (Corning, Corning, NY, USA) were used to evaluate cell invasion *in vitro*. Cells, serum-starved for 24 h, were first suspended in serum-free RPMI-1640 to a final cell density of 5 $\times$ $10^5$ cells·$mL^{-1}$ in the invasion assay. A 1-mL cell suspension was seeded into the top chamber, lined with a membrane coated with 200 mg·$mL^{-1}$ Matrigel (BD Biosciences, San Jose, CA, USA), and the lower chamber beneath the polycarbonate membranes was filled with 2.5 mL of RPMI-1640 medium supplemented with 20% fetal bovine serum, which was used as a chemoattractant for the cells. After incubation at 37 °C for 48 h after seeding, the cells on the upper surface of the membrane were wiped with cotton wool. Cell monolayers on the underside of the membrane were fixed in 100% methanol for 10 min, and stained with 0.1% crystal violet. Three visual fields of each chamber were randomly counted under a microscope (with 20 $\times$ 10 lenses). The means of triplicate assays for each experimental condition were used.

## Western blot analysis

Lung cancer cells were transfected with miR-133b mimic, inhibitor or miR-NC in six-well plates (1.0 $\times$ $10^6$ cells per

well). After being incubated at 37 °C for 48 h, cells were lysed in ice-cold lysis buffer containing 50 mM Tris/HCl (pH 7.4), 150 mM NaCl, 1% NP-40, 1 mM phenylmethanesulfonyl fluoride, 1 mM EDTA, and complete proteinase inhibitor mixture. After protein content determination with a bicinchoninic acid Protein Assay Kit (Keygen Biotech), standard western blotting was performed with antibodies as described above, according to the manufacturer's instructions. The optimal antibody dilutions were 1 : 1000, 1 : 1000, 1 : 500, 1 : 200 and 1 : 1000 for mAb against EGFR, mAb against pEGFR, polyclonal antibody against pERK1/2, polyclonal antibody against pAKT1/2/3, and mAb against β-actin, respectively.

### Statistical analysis

All data shown are mean ± standard deviation (SD), if not stated otherwise. Statistical analysis of the data was performed by applying Student's *t*-test. Associations of miR-133b with *EGFR* mRNA expression levels and the other risk factors were calculated for all tumor samples with chi-squared tests and bivariate Spearman rank correlation analysis. Overall survival was estimated with the Kaplan–Meier method, and the resulting curves were compared by use of the log-rank test. Overall survival was calculated as the interval between the date of lung cancer surgery and either the date of death or the date of the last clinical follow-up. The results of cell proliferation, apoptosis, qRT-PCR and western blotting were analyzed with one-way ANOVA. All *P*-values were two-sided, and $P < 0.05$ was considered to be statistically significant. Statistical computations were performed with SPSS v13.0 (SPSS, Chicago, IL, USA) and GRAPHPAD v5.0 (GraphPad, San Diego, CA, USA).

## Acknowledgements

This work was supported by the Clinical Oncology Research Program of Medical Science and the Technology Development Foundation in Health Department of Jiangsu Province (P200905) and the National Natural Science Foundation of China (81071643, 81172140). We thank Z. Tao and W. Zhu for excellent technical assistance. We thank J. Xu for advice regarding the qRT-PCR.

## References

1 Jemal A, Siegel R, Xu J & Ward E (2010) Cancer statistics, 2010. *CA Cancer J Clin* **60**, 277–300.
2 Murphy M & Stordal B (2011) Erlotinib or gefitinib for the treatment of relapsed platinum pretreated non-small cell lung cancer and ovarian cancer: a systematic review. *Drug Resist Updat* **14**, 177–190.
3 Liang Z, Zhang J, Zeng X, Gao J, Wu S & Liu T (2010) Relationship between EGFR expression, copy number and mutation in lung adenocarcinomas. *BMC Cancer* **10**, 376–384.
4 Hirsch FR, Varella-Garcia M, Cappuzzo F, McCoy J, Bemis L, Xavier AC, Dziadziuszko R, Gumerlock P, Chansky K, West H *et al.* (2007) Combination of EGFR gene copy number and protein expression predicts outcome for advanced non-small-cell lung cancer patients treated with gefitinib. *Ann Oncol* **18**, 752–760.
5 Mathonnet G, Fabian MR, Svitkin YV, Parsyan A, Huck L, Murata T, Biffo S, Merrick WC, Darzynkiewicz E, Pillai RS *et al.* (2007) MicroRNA inhibition of translation initiation in vitro by targeting the cap-binding complex eIF4F. *Science*, **317**, 1764–1767.
6 Weiss GJ, Bemis LT, Nakajima E, Sugita M, Birks DK, Robinson WA, Varella-Garcia M, Bunn PA Jr, Haney J, Helfrich BA *et al.* (2008) EGFR regulation by microRNA in lung cancer: correlation with clinical response and survival to gefitinib and EGFR expression in cell lines. *Ann Oncol* **19**, 1053–1059.
7 Tavazoie SF, Alarcon C, Oskarsson T, Padua D, Wang Q, Bos PD, Gerald WL & Massague J (2008) Endogenous human microRNAs that suppress breast cancer metastasis. *Nature* **451**, 147–152.
8 Calin GA, Ferracin M, Cimmino A, Di Leva G, Shimizu M, Wojcik SE, Iorio MV, Visone R, Sever NI, Fabbri M *et al.* (2005) A microRNA signature associated with prognosis and progression in chronic lymphocytic leukemia. *N Engl J Med* **353**, 1793–1801.
9 Nagel R, le Sage C, Diosdado B, van der Waal M, Oude Vrielink JA, Bolijn A, Meijer GA & Agami R (2008) Regulation of the adenomatous polyposis coli gene by the miR-135 family in colorectal cancer. *Cancer Res* **68**, 5795–5802.
10 Li W, Xie L, He X, Li J, Tu K, Wei L, Wu J, Guo Y, Ma X, Zhang P *et al.* (2008) Diagnostic and prognostic implications of microRNAs in human hepatocellular carcinoma. *Int J Cancer* **123**, 1616–1622.
11 Bloomston M, Frankel WL, Petrocca F, Volinia S, Alder H, Hagan JP, Liu CG, Bhatt D, Taccioli C & Croce CM (2007) MicroRNA expression patterns to differentiate pancreatic adenocarcinoma from normal pancreas and chronic pancreatitis. *JAMA* **297**, 1901–1908.
12 Porkka KP, Pfeiffer MJ, Waltering KK, Vessella RL, Tammela TL & Visakorpi T (2007) MicroRNA expression profiling in prostate cancer. *Cancer Res* **67**, 6130–6135.
13 Weidhaas JB, Babar I, Nallur SM, Trang P, Roush S, Boehm M, Gillespie E & Slack FJ (2007) MicroRNAs as potential agents to alter resistance to cytotoxic anticancer therapy. *Cancer Res* **67**, 11111–11116.

14 Wang Y, Wang X, Zhang J, Sun G, Luo H, Kang C, Pu P, Jiang T, Liu N & You Y (2012) MicroRNAs involved in the EGFR/PTEN/AKT pathway in gliomas. *J Neurooncol* **106**, 217–224.
15 Kang JU, Koo SH, Kwon KC, Park JW, Shin SY, Kim JM & Jung SS (2007) High frequency of genetic alterations in non-small cell lung cancer detected by multi-target fluorescence in situ hybridization. *J Korean Med Sci* **22**(Suppl), S47–S51.
16 Crawford M, Batte K, Yu L, Wu X, Nuovo GJ, Marsh CB, Otterson GA & Nana-Sinkam SP (2009) MicroRNA 133B targets pro-survival molecules MCL-1 and BCL2L2 in lung cancer. *Biochem Biophys Res Commun* **388**, 483–489.
17 de Mena L, Coto E, Cardo LF, Diaz M, Blazquez M, Ribacoba R, Salvador C, Pastor P, Samaranch L, Moris G *et al.* (2010) Analysis of the micro-RNA-133 and PITX3 genes in Parkinson's disease. *Am J Med Genet B Neuropsychiatr Genet* **153B**, 1234–1239.
18 Xiao L, Xiao J, Luo X, Lin H, Wang Z & Nattel S (2008) Feedback remodeling of cardiac potassium current expression: a novel potential mechanism for control of repolarization reserve. *Circulation* **118**, 983–992.
19 Koutsoulidou A, Mastroyiannopoulos NP, Furling D, Uney JB & Phylactou LA (2011) Expression of miR-1, miR-133a, miR-133b and miR-206 increases during development of human skeletal muscle. *BMC Dev Biol* **11**, 34–42.
20 Zeiger U & Khurana TS (2010) Distinctive patterns of microRNA expression in extraocular muscles. *Physiol Genomics* **41**, 289–296.
21 Kozakowska M, Ciesla M, Stefanska A, Skrzypek K, Was H, Jazwa A, Grochot-Przeczek A, Kotlinowski J, Szymula A, Bartelik A *et al.* (2012) Heme oxygenase-1 inhibits myoblast differentiation by targeting myomirs. *Antioxid Redox Signal* **16**, 113–127.
22 Palmieri A, Pezzetti F, Brunelli G, Zollino I, Scapoli L, Martinelli M, Arlotti M & Carinci F (2007) Differences in osteoblast miRNA induced by cell binding domain of collagen and silicate-based synthetic bone. *J Biomed Sci* **14**, 777–782.
23 Haas JD, Nistala K, Petermann F, Saran N, Chennupati V, Schmitz S, Korn T, Wedderburn LR, Forster R, Krueger A *et al.* (2011) Expression of miRNAs miR-133b and miR-206 in the Il17a/f locus is co-regulated with IL-17 production in alphabeta and gammadelta T cells. *PLoS One* **6**, e20171.
24 Widera C, Gupta SK, Lorenzen JM, Bang C, Bauersachs J, Bethmann K, Kempf T, Wollert KC & Thum T (2011) Diagnostic and prognostic impact of six circulating microRNAs in acute coronary syndrome. *J Mol Cell Cardiol* **51**, 872–875.
25 Wu Y, Crawford M, Yu B, Mao Y, Nana-Sinkam SP & Lee LJ (2011) MicroRNA delivery by cationic lipoplexes for lung cancer therapy. *Mol Pharm* **8**, 1381–1389.
26 Kano M, Seki N, Kikkawa N, Fujimura L, Hoshino I, Akutsu Y, Chiyomaru T, Enokida H, Nakagawa M & Matsubara H (2010) miR-145, miR-133a and miR-133b: tumor suppressive miRNAs target FSCN1 in esophageal squamous cell carcinoma. *Int J Cancer* **127**, 2804–2814.
27 Akcakaya P, Ekelund S, Kolosenko I, Caramuta S, Ozata DM, Xie H, Lindforss U, Olivecrona H & Lui WO (2011) miR-185 and miR-133b deregulation is associated with overall survival and metastasis in colorectal cancer. *Int J Oncol* **39**, 311–318.
28 Guo J, Miao Y, Xiao B, Huan R, Jiang Z, Meng D & Wang Y (2009) Differential expression of microRNA species in human gastric cancer versus non-tumorous tissues. *J Gastroenterol Hepatol* **24**, 652–657.
29 Song T, Xia W, Shao N, Zhang X, Wang C, Wu Y, Dong J, Cai W & Li H (2010) Differential miRNA expression profiles in bladder urothelial carcinomas. *Asian Pac J Cancer Prev* **11**, 905–911.
30 Wong TS, Liu XB, Chung-Wai Ho A, Po-Wing Yuen A, Wai-Man Ng R & Ignace Wei W (2008) Identification of pyruvate kinase type M2 as potential oncoprotein in squamous cell carcinoma of tongue through microRNA profiling. *Int J Cancer* **123**, 251–257.
31 Qin W, Dong P, Ma C, Mitchelson K, Deng T, Zhang L, Sun Y, Feng X, Ding Y, Lu X *et al.* (2011) MicroRNA-133b is a key promoter of cervical carcinoma development through the activation of the ERK and AKT1 pathways. *Oncogene* in press, doi:10.1038/onc.2011.561.
32 Navon R, Wang H, Steinfeld I, Tsalenko A, Ben-Dor A & Yakhini Z (2009) Novel rank-based statistical methods reveal microRNAs with differential expression in multiple cancer types. *PLoS One* **4**, e8003.
33 Hu G, Chen D, Li X, Yang K, Wang H & Wu W (2010) miR-133b regulates the MET proto-oncogene and inhibits the growth of colorectal cancer cells in vitro and in vivo. *Cancer Biol Ther* **10**, 190–197.
34 Du L & Pertsemlidis A (2011) Cancer and neurodegenerative disorders: pathogenic convergence through microRNA regulation. *J Mol Cell Biol* **3**, 176–180.
35 Brodersen P & Voinnet O (2009) Revisiting the principles of microRNA target recognition and mode of action. *Nat Rev Mol Cell Biol* **10**, 141–148.
36 Jorissen RN, Walker F, Pouliot N, Garrett TP, Ward CW & Burgess AW (2003) Epidermal growth factor receptor: mechanisms of activation and signalling. *Exp Cell Res* **284**, 31–53.
37 Ogata T, Teshima T, Inaoka M, Minami K, Tsuchiya T, Isono M, Furusawa Y & Matsuura N (2011) Carbon ion irradiation suppresses metastatic potential of human non-small cell lung cancer A549 cells through

the phosphatidylinositol-3-kinase/Akt signaling pathway. *J Radiat Res* **52**, 374–379.
38 Mercer KE & Pritchard CA (2003) Raf proteins and cancer: B-Raf is identified as a mutational target. *Biochim Biophys Acta* **1653**, 25–40.
39 Langlois B, Perrot G, Schneider C, Henriet P, Emonard H, Martiny L & Dedieu S (2010) LRP-1 promotes cancer cell invasion by supporting ERK and inhibiting JNK signaling pathways. *PLoS One* **5**, e11584.
40 Cappuzzo F, Magrini E, Ceresoli GL, Bartolini S, Rossi E, Ludovini V, Gregorc V, Ligorio C, Cancellieri A, Damiani S *et al.* (2004) Akt phosphorylation and gefitinib efficacy in patients with advanced non-small-cell lung cancer. *J Natl Cancer Inst* **96**, 1133–1141.
41 Paez JG, Janne PA, Lee JC, Tracy S, Greulich H, Gabriel S, Herman P, Kaye FJ, Lindeman N, Boggon TJ, *et al.* (2004) EGFR mutations in lung cancer: correlation with clinical response to gefitinib therapy. *Science* **304**, 1497–1500.
42 Weinstein IB (2002) Cancer. Addiction to oncogenes – the Achilles heal of cancer. *Science* **297**, 63–64.
43 Pietanza MC, Lynch TJ Jr, Lara PN Jr, Cho J, Yanagihara RH, Vrindavanam N, Chowhan NM, Gadgeel SM, Pennell NA, Funke R, *et al.* (2012) XL647-A multitargeted tyrosine kinase inhibitor: results of a phase II study in subjects with non-small cell lung cancer who have progressed after responding to treatment with either gefitinib or erlotinib. *J Thorac Oncol* **7**, 219–226.
44 Spigel D, Ervin T, Ramlau R, Daniel D, Goldschmidt J, Blumenschein G, Krzakowski M, Robinet G, Clement-Duchene C & Barlesi F (2011) Final efficacy results from OAM4558g, a randomized phase II study evaluating MetMAb or placebo in combination with erlotinib in advanced NSCLC. *J Clin Oncol* **29**, Abstract No. 7505.
45 Goldstraw P, Crowley J, Chansky K, Giroux DJ, Groome PA, Rami-Porta R, Postmus PE, Rusch V & Sobin L (2007) The IASLC Lung Cancer Staging Project: proposals for the revision of the TNM stage groupings in the forthcoming (seventh) edition of the TNM classification of malignant tumours. *J Thorac Oncol* **2**, 706–714.
46 Travis WD, Colby TV, Corrin B, Shimosato Y, Brambilla E & Sobin LH (1999) Histological Typing of Lung and Pleural Tumours, 3rd edn. Berlin, Springer-Verlag.
47 Thomson S, Buck E, Petti F, Griffin G, Brown E, Ramnarine N, Iwata KK, Gibson N & Haley JD (2005) Epithelial to mesenchymal transition is a determinant of sensitivity of non-small-cell lung carcinoma cell lines and xenografts to epidermal growth factor receptor inhibition. *Cancer Res* **65**, 9455–9462.
48 Sordella R, Bell DW, Haber DA & Settleman J (2004) Gefitinib-sensitizing EGFR mutations in lung cancer activate anti-apoptotic pathways. *Science* **305**, 1163–1167.
49 Livak KJ & Schmittgen TD (2001) Analysis of relative gene expression data using real-time quantitative PCR and the 2(-Delta Delta C(T)) method. *Methods* **25**, 402–408.
50 Pfaffl MW (2001) A new mathematical model for relative quantification in real-time RT-PCR. *Nucleic Acids Res* **29**, 2002–2007.

## Supporting information

The following supplementary material is available:
**Fig. S1.** Expression of miR-133b was suppressed in non-small-cell lung cancer cancer detected by *in situ* hybridization.
**Fig. S2.** Kaplan–Meier estimates of overall survival times of patients with non-small-cell lung cancer according to miR-133b relative expression.
**Fig. S3.** MiR-133b targets *EGFR* mRNA by binding to the EGFR 3′-UTR.
**Fig. S4.** MiR-133b was regulated by liposomal delivery of mimic or inhibitor.
**Fig. S5.** Summary of the molecular events related to the upregulation of miR-133b that results in cellular phenotype changes of human cancer.
**Table S1.** Comparison of several clinicopathological factors and expression levels of miR-133b in non-small-cell lung cancer specimens (Spearman rank correlation tests).
**Table S2.** The functional distribution and the significantly enriched functional categories of other cancer-related genes targeted by miR-133b.
**Table S3.** Sequences of primers used for RT-PCR analysis of gene expression.

This supplementary material can be found in the online version of this article.

Please note: As a service to our authors and readers, this journal provides supporting information supplied by the authors. Such materials are peer-reviewed and may be reorganized for online delivery, but are not copy-edited or typeset. Technical support issues arising from supporting information (other than missing files) should be addressed to the authors.